

Development Phases and Mechanisms of Tectonic Fractures in the Longmaxi Formation Shale of the Dingshan Area in Southeast Sichuan Basin, China

FAN Cunhui^{1,2,3}, HE Shun^{1,3}, ZHANG Yu^{1,3}, QIN Qirong^{1,2,3,*} and ZHONG Cheng^{1,3}

1 *State Key Laboratory of Oil and Gas Reservoir Geology and Exploitation, Southwest Petroleum University, Chengdu 610500, China*

2 *State Key Laboratory of Oil and Gas Reservoir Geology and Exploitation, Chengdu University of Technology, Chengdu 610059, China*

3 *School of Geoscience and Technology, Southwest Petroleum University, Chengdu 610500, China*

Abstract: Shale gas has currently attracted much attention during oil and gas exploration and development. Fractures in shale have an important influence on the enrichment and preservation of shale gas. This work studied the developmental period and formation mechanism of tectonic fractures in the Longmaxi Formation shale in the Dingshan area of southeastern Sichuan Basin based on extensive observations of outcrops and cores, rock acoustic emission (Kaiser) experiments, homogenization temperature of fracture fill inclusions, apatite fission track, thermal burial history. The research shows that the fracture types of the Longmaxi Formation include tectonic fractures, diagenetic fractures and horizontal slip fractures. The main types are tectonic high-angle shear and horizontal slip fractures, with small openings, large spacing, low densities, and high degrees of filling. Six dominant directions of the fractures after correction by plane included NWW, nearly SN, NNW, NEE, nearly EW and NW. The analysis of field fracture stage and fracture system of the borehole suggests that the fractures in the Longmaxi Formation could be paired with two sets of plane X-shaped conjugate shear fractures, i.e., profile X-shaped conjugate shear fractures and extension fractures. The combination of qualitative geological analysis and quantitative experimental testing techniques indicates that the tectonic fractures in the Longmaxi Formation have undergone three periods of tectonic movement, namely mid-late Yanshanian movement (82–71.1 Ma), late Yanshanian and middle Himalaya movements (71.1–22.3 Ma), and the late Himalayan movement (22.3–0 Ma). The middle-late period of the Yanshanian movement and end of the Yanshanian movement-middle period of the Himalayan movement were the main fracture-forming periods. The fractures were mostly filled with minerals, such as calcite and siliceous. The homogenization temperature of fracture fill inclusions was high, and the paleo-stress value was large; the tectonic movement from the late to present period was mainly a slight transformation and superposition of existing fractures and tectonic systems. Based on the principle of tectonic analysis and theory of geomechanics, we clarified the mechanism of the fractures in the Longmaxi Formation, and established the genetic model of the Longmaxi Formation. The research on the qualitative and quantitative techniques of the fracture-phase study could be effectively used to analyze the causes of the marine shale gas fractures in the Sichuan Basin. The research findings and results provide important references and technical support for further exploration and development of marine shale gas in South China.

Key words: shale, fracture characteristics, formation phases, Longmaxi Formation, Dingshan area, Sichuan Basin

1 Introduction

North America has greatly benefited from the

exploration and development of shale gas resources (Curtis, 2002; Bustin, 2005; Montgomery, 2005; Martinesu, 2007; Nelson, 2011; Ambrose et al., 2012; Nie Haikuang and Zhang Jinchuan, 2012; Zou Caineng et al.,

* Corresponding author. E-mail: 986336692@qq.com

2015; Jarvie et al., 2017). Since 2005, China has also strengthened the exploration and development of shale gas. In the Sichuan Basin, some shale gas fields with commercial value were discovered, such as the Fuling, Weiyuan, Changning and Zhaotong fields, the largest among them being the Fuling shale gas field with proved reserves up to $3805.98 \times 10^8 \text{ m}^3$, making it the second largest shale gas field in the world following that in North America (Guo Xusheng et al., 2014; Feng Ziqi et al., 2016). With a current production capacity of $100 \times 10^8 \text{ m}^3$, the Fuling shale gas field has far-reaching significance in promoting the rapid development of China's natural gas industry and ensuring national energy security (Zou Caineng et al., 2015). It has been proven by the exploration and development of shale gas nationally and internationally that shale fractures or fracture networks formed after fracturing have great significance for the enrichment of shale gas and the improvement of reservoir performance and production capacity (Pedersen and Calvert, 1990; Narr, 1991; Rodriguez and Philp, 2010; Zumberge et al., 2012; Hao, 2013; Guo Xusheng et al., 2014; Wang Ke et al., 2016; Feng Dongjun et al., 2016; Zou Caineng et al., 2016).

Owing to the effect of tectonic stress, various types of fractures are easily generated in shale. In general, gas reservoirs with a higher degree of fracture development have better quality (Pedersen and Calvert, 1990; Narr, 1991; Rodriguez and Philp, 2010; Zumberge et al., 2012; Hao, 2013; Zou Caineng et al., 2016). The productivity of shale gas in the Longmaxi Formation of the Sichuan Basin is closely related to the development of fractures (Nelson, 2001; Awdal et al., 2013; Gale et al., 2014; Fan Cunhui et al., 2016; Zou Caineng et al., 2016; Wang Ruyue et al., 2016). The history of the formation development and evolution of tectonic fractures is an important factor in oil and gas exploration and development. The characteristics of tectonic fractures, formation period, and genesis mechanisms are the focus and difficulties that need to be overcome in the field (Nelson, 2001; Larsen et al., 2012; Awdal et al., 2013; Gale et al., 2014; Fan Cunhui et al., 2016, 2017; Zou Caineng et al., 2016; Wang Ke et al., 2016; Lü Jing et al., 2017; Yuan Yusong et al., 2017). There are a variety of methods to study tectonic fractures, including data observation on outcrops and core fractures, analytical analysis on downhole fault structure, rock acoustic emission experiments, homogeneous temperature tests of fracture fillings inclusions, and apatite fission track test results.

The Dingshan area is located in Qijiang in the southeast of the Sichuan Basin, attached to Shihao town, Chongqing, covering an area of about 440 km^2 . Recently, great advancements have been made in Dingshan in the

exploration of tectonic shale gas, and the key exploratory well (well 4) for gas testing of shale gas has the highest daily production of $20.56 \times 10^4 \text{ m}^3$, confirming that the Dingshan area has good exploration and development prospects of shale gas. Under the effect of tectonic stress, well-developed tectonic fractures have formed in the Longmaxi Formation shale owing to the ductile shear rupture. The research area has undergone tectonic movement transformations of the Caledonian, Indosinian, Yanshanian, and Himalayan phases (Yuan Haifeng, 2008; Ding Wenlong et al., 2012; Hu Dongfeng et al., 2014; Lu Yingxin et al., 2016). The tectonic fractures of different phases have an important effect on the preservation and enrichment of shale gas, and the shale gas production of the Dingshan area, southeastern Sichuan. Therefore, this paper took the tectonic shale of the Longmaxi Formation of the Dingshan area in southeastern Sichuan as a case to comprehensively study fracture formation phases and clarify the development phases and evolution modes to further guide the exploration and development of shale gas in the Longmaxi Formation, based on fracture investigations of surface outcrops, structural analysis, observation of well drilling cores, and imaging logging explanations, combined with inclusion analyses of fracture fillings, rock acoustic emission experiments, apatite fission tracks (Sonntag et al., 2012), burial history analyses, and previous research results.

2 Geological Settings

The Dingshan tectonic area is located in the down-warping folded region in southeastern Sichuan, and the southern part spans the joint position of the eastern margin of the low belt of folded strata South of Sichuan and the southern slope belt of the Sichuan Basin. It has a potential height (Sun Wei et al., 2014) of the blind fault footwall at the anticlinal northwest wing of Jiudianya. With the whole plane modality manifesting as a nose-like anticline in an NE-SW direction, the Dingshan area lies in the Sangmuchang–Jiudianya tectonic belt, where most linear folds exist. The main structure is a trough-like fold constituted by a high-steep anticline and fault belt of NE and NNE directions, and the tectonic pattern is anticlinal, wide and low, synclinal and compact, arranged in a parallel arrangement (Fig. 1).

The lower part of the Longmaxi Formation in the Dingshan area is dominated by carbonaceous and arenaceous shale; the upper part is an interbedding of calcareous shale and laminated argillaceous apatite; and is about 158–334 m thick, and generally about 250 m long. It can be divided into the upper and lower sections according to the lithology. The lower section is graptolite shale, and

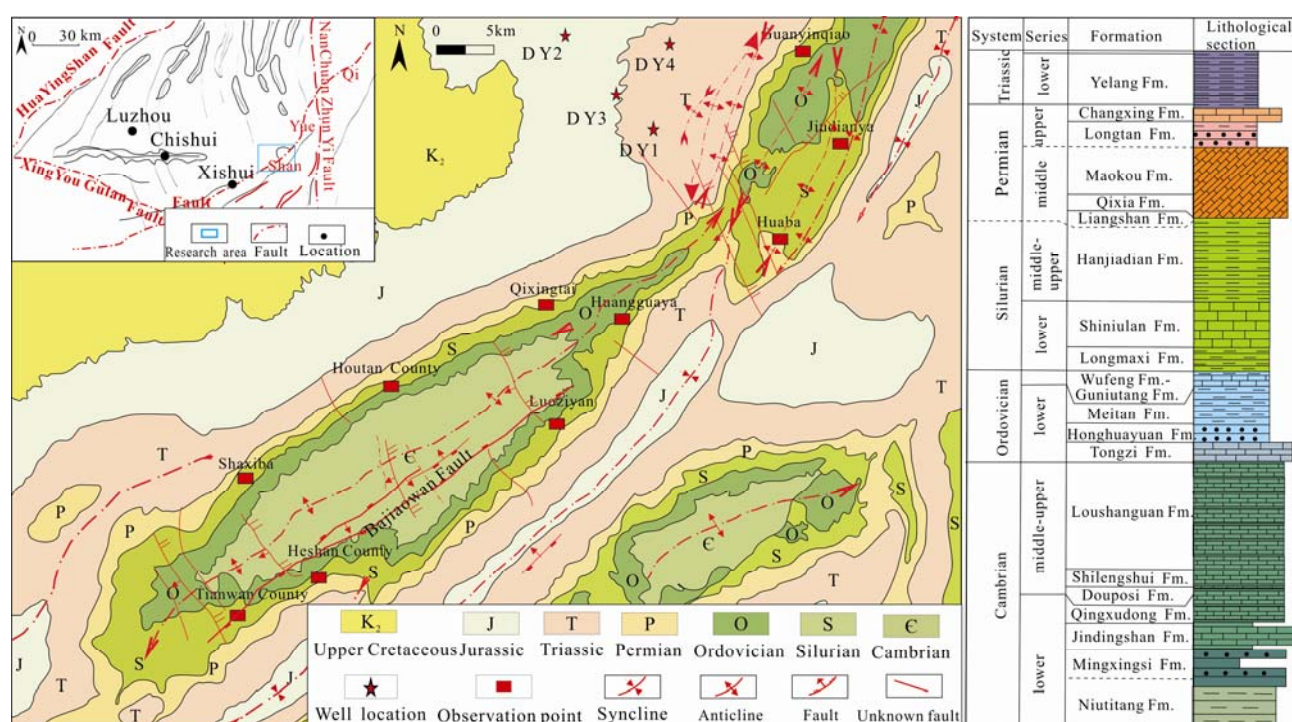


Fig. 1. Simplified regional geological map of the study area.

1, Upper Cretaceous; 2, Jurassic; 3, Triassic; 4, Permian; 5, Silurian; 6, Ordovician; 7, Cambrian; 8, Sinian; 9, dorsal syncline; 10, faults; 11, structural fractures and unidentified faults; 12, well locations.

the upper section is the interbedding of gray-dark gray calcareous shale, calcilutite and gray laminated argillaceous apatite or marlstone (the lower section is calcareous shale and argillaceous apatite, and the upper section is the interbedding of calcareous shale and argillaceous apatite), locally being calcareous sandstone.

3 Samples and Methods

In this study, fracturing episodes and mechanisms were determined mainly through geological and experimental methods. Geological methods included geological field surveys and measurements of fractures, analyses of coring and logging data and experimental tests. Experimental tests were based on three methods, namely, the homogenization temperature measurements on inclusions in fracture fillings, analyses of apatite fission-track ages and burial history, and Kaiser effect stresses of rocks.

3.1 Geological measure and date analyses

Geological surveys were conducted mainly on the Longmaxi Formation around Jiudianya and Sangmuchang. There were ten surveying routes in total. Fracturing episodes were determined mainly by the development, cross-cutting relationships, and geometry of fractures in the field. Analyses of the coring and logging data were based on the data from five 460-m wells. According to the filling characteristics, cross-cutting relationships, and

geometry of the fractures, the formation episodes of subsurface fractures were deduced. Tectonic interpretation and analyses mainly utilized three-dimensional seismic data to resolve the distribution and mutually constraining relationships of faults in the Longmaxi Formation underground. Formation of faults and fractures were correlated mechanically. Resolution of faults revealed stages of tectonic evolution and thereby validated the fracture-forming episodes. It is a practical and reliable method to invert the paleo-structure stress fields based on rich experience and traditional reliable tectonic theory and means (Nai Haikuang et al., 2004; Deng Bin et al., 2009; Xu Kangkang et al., 2012; Bai Bin et al., 2012; Dai Junsheng et al., 2017; Li Yufeng et al., 2018). This paper took the developed fractures in the exposed Longmaxi Formation stratum in the Dingshan area as the object of study, and obtained more than 600 directional observation data from the outcrop areas, including Guanyinqiao, Huaba, and Jiudianya (Fig. 2; Table 1).

3.2 Experimental tests

To understand the fracture formation phases, the homogeneous temperature test was performed on the test sample of the Longmaxi Formation in the Dingshan area.

The fracture filling inclusions analysis technique is an effective method, which mainly adopts the homogenous temperature of primary inclusions formed at the same time of fracture filling to infer the paleo-structure period when

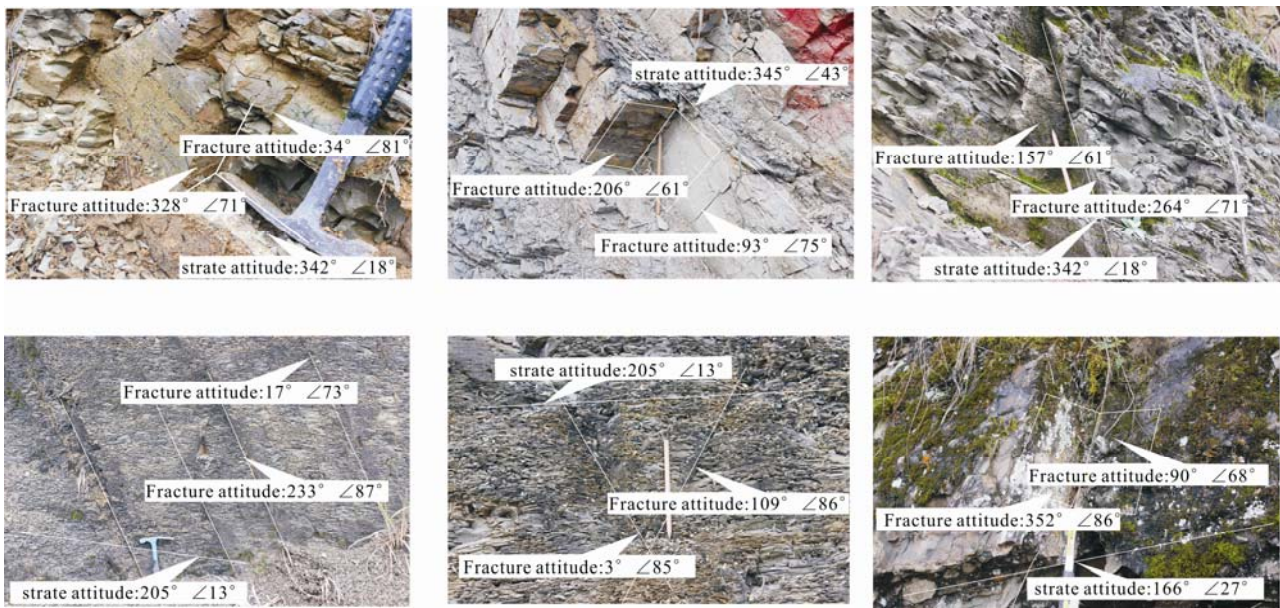


Fig. 2. Structural fractures of the Longmaxi Formation in the study area.

fractures formed (Zheng Rongcai et al., 1998; Anderson, 1948; Newton, 1990; Ren Lihua and Lin Changyan, 2007; Yang Wei et al., 1996; Nai Shenghua et al., 2004; Deng Bin et al., 2009; Bao Hongzhi et al., 2009; Li Zhongquan and Liu Shun, 2010; Zhang Xufeng et al., 2010; Xu Kangkang et al., 2012; Bai Bin et al., 2012; Dai Peng et al., 2015; Li Yang et al., 2016; Feng Dongjun et al., 2016; Niu Hairui et al., 2017; Dai Junsheng et al., 2017). Apatite fission track technology is not only a dating technique, but also an analysis technique for thermal evolution history. The track age and length distribution of apatite is considered to comprehensively reflect the thermal history, and can restore the thermal history (Xu Kangkang et al., 2012). Thus, apatite fission tracks have become an important and unique source of information for obtaining the thermal history and tectonic evolution of low-temperature regions. The rocks showed the Kaiser effect and acoustic emission experiments could be performed to observe the fracture phases. When the stress value of the rock load reached the quantity of the paleo stress field, micro-fractures were reopened, forming the Kaiser effect point (Nai Shenghua et al., 2004; Bao Hongzhi et al., 2009; Zhang Jinhang et al., 2010; Bai Bin et al., 2012; Li Yang et al., 2016; Zhao Jianhua et al., 2016). The stress phases and tectonic stress field intensity of the rocks could be interpreted with the Kaiser effect point found by the acoustic emission experiment.

To accurately determine the uplift and settlement history (the tectonic evolution history) of the Longmaxi Formation in the Dingshan area, the formation time of the Longmaxi Formation fractures was defined chronologically. In the present study, a more accurate

dating method, apatite fission track technology, was adopted to invert the uplift history of the study area since the late Yanshanian period.

In the present study, the high temperature and high pressure triaxial rock mechanics test system RTR-1000 (GCTS company) was adopted to perform the rock mechanics parameters experiment, the Kaiser effect test was conducted on the five core samples of DY3, DY4, and DY5 wells, and the acoustic emission experiment was carried out on the core samples from the three angles of 0, 45, and 90°, determining the time corresponding to the original data of energy, ringing coefficient, and intensity.

4 Results

4.1 Fracture characteristics

4.1.1 Fracture types

According to the core observation of the five wells, including DY1, DY2, DY3, DY4, and DY5, combined with the fracture analysis of the outcrops, such as Chongqing Guanyinqiao, Huaba, and Jiudianya, the fractures of the Longmaxi Formation in the Dingshan area could be divided into tectonic, diagenetic, and horizontal detachment fractures, and mainly consisted of structural fractures. Structural fractures mainly include plane shear, section shear, and a small number of tensile fractures. The shear fractures are widely developed. Shear fractures are generally developed at the observation sites of the anticline nucleus and two wings and usually appear in pairs. The depth of cut through is large, and the developed filling minerals have significant directionality. The extension fractures had short extension distances, a

Table 1 List of tectonic fractures on outcrops of the Longmaxi Formation shale in the Dingshan-Sangmuchi area

Location	strate attitude	Partial date of dominant attitude		Strike rose diagram of fracture(after attitude recover)	The overall strike rose diagram of fractures in the study area (after sttitude recovery)
		Plane shear fracture	Section shear fracture		
Jiudianya	250° ∠13°	34° ∠80° 154° ∠84°	306° ∠64°		<p>Strike rose diagram of fractures in the Longmaxi Formation (surface)</p> <p>Inversion of force diagram The dominant direction of plane shear fractures: ① NWW(295° ± 5°) ② SN(5 ± 5°) ③ NNW(345 ± 5°) ④ WE(85 ± 5°)</p> <p>The dominant direction of section shear fractures: ① NE(35 ± 5°) ② NW(315 ± 5°)</p>
Huanggua ya	166° ∠27°	15° ∠87° 85° ∠75° 76° ∠85°	129° ∠77°		
Qixingtai	343° ∠24°	120° ∠54° 126° ∠80°	48° ∠62°		
HouTan	345° ∠43°	145° ∠79°	307° ∠65°		
HuanBa	342° ∠18°	43° ∠74° 328° ∠90°	228° ∠69°		
ShaXiBa	315° ∠15°	35° ∠81° 65° ∠68°	122° ∠64°		
TianWan	315° ∠15°	189° ∠90° 95° ∠89° 277° ∠86°	126° ∠68°		
HeShan	162° ∠27°	256° ∠82°	47° ∠69°		
LuoZiYan	175° ∠21°	85° ∠81° 45° ∠78°	227° ∠42°		
GuanYin Qiao	312° ∠25°	252° ∠77° 175° ∠73° 105° ∠85°	315° ∠82°		

tortuous tail was partially visible in the core (Fig. 2c), and extension fractures on the surface were mainly developed in the anticline nucleus, spreading along the direction of the junction (NE direction). The diagenetic fractures were mainly developed at the lithologic interface, especially at the interface of the argillaceous rocks, and usually developed along the bedding plane. The horizontal slip fractures had a low degree of angle, and scratch marks and flat friction mirrors could be seen locally. In addition, artificially induced fractures in the drilling process owing

to the imbalance of heavy mud and ground stress and drill load and torsion were visible in the core.

4.1.2 Fracture development characteristics

According to the observation and statistics of the five well cores and surface, the Longmaxi Formation in the Dingshan area had fractures with lengths of mainly 10–20 cm, followed by those ≥ 20 cm, and the two types of fractures accounted for about 90% of the total fractures. The fracture width was mainly concentrated at 0.5–1 mm,

accounting for 50%, followed by those at <0.5 mm, accounting for about 14%, and generally the area was mainly distributed with small-width fractures, which were relatively closed. The fracture extension length was concentrated in a range of 10–20 cm, of medium degree. The fracture density was mainly concentrated in 1–1.5 fractures/m, 0.5–1 fractures/m, < 0.5 fractures/m, respectively, accounting for 23%, 33%, and 21% of the fracture development section. The fracture density of this area was relatively small, mostly lower than 1.5/m (Fig. 3).

In the Dingshan area, the length of the core fractures in the Longmaxi formation was mainly 10–20 cm, followed by fractures with a length of ≥ 20 cm, both kinds of fractures accounted for approximately 90% of the total number of fractures. The fracture angles were horizontal ($<15^\circ$) and vertical (75° – 90°), accounting for 31% and 56%, respectively. The cores were mainly high-angle shear fractures and horizontal slip fractures; the fracture widths were mainly concentrated between 0.5–1 mm, accounting for 50%, followed by fractures with a width of <0.5 mm accounting for about 14%. Overall, fractures in this area were dominated by small relatively closed fractures; fracture density was mainly concentrated in 1–1.5 bars/m, 0.5–1 bars/m, and <0.5 bars/m, accounting for 23%, 33%, and 21% of all fracture development zones, respectively, and the density was generally small (Fig. 3). According to core observations and FMI logging data, the proportion of unfilled fractures in the reservoir fractures of the Longmaxi Formation was about 20%, half-filled fractures was about 20%, full-filled fractures was about 60%. The filling materials for filling fractures included calcite, pyrite, and organic matter. The filling degree was high, reflecting the good sealing effect of fractures in this area. The surface fractures were dominated by tectonic

fractures, with large dip angles, often intersecting with stratum at high angles. The fracture characteristics differed significantly from those of cores; the extension of surface fractures was relatively long, and the surface fractures had long extensions, 60% of the extension length was between 0.5 and 2 m, and 20% was between 2 and 4 m; fractures were mainly developed with medium densities (3–8 bars/m), followed by <3 bars/m, both accounting for 95% of the total number of fractures, and the line density was higher than that of the fractures in the core.

The fracture development degree of the Longmaxi Formation was impacted by the factors such as tectonic location, mineral composition, rock thickness, and rock mechanical parameters. The tectonic type of the study area was mainly the thrust-nappe structure formed and controlled by the blind fault at the leading edge of Qiyueshan Mountain, which mainly develops folds and fractures in NE, NS, and NW directions. The shale in the study area had a brittle mineral content of 52.3%–62.6%, carbonatite content of 15.4%–21.6%, and clay mineral content of 20.4%–32.0%, with a brittleness index of 52.30–62.66, 57.35 on average, i.e., an above-average level, so the fracture development was relatively good; the elasticity modulus of the Longmaxi Formation fracture was determined as 31746–20632 MPa and the Poisson's ratio was 0.171–0.195 through triaxial stress tests, implying that shale has a good capacity of fracture-making, with excellent fracture toughness.

4.2 Fracture development phases

4.2.1 Investigation of ground surface fractures and classification of fracture phases

The stratigraphic dip changed and the occurrence shape of fractures formed earlier also changed under the effect of stress superposition. The fracture occurrence shape by the



Fig. 3. Characteristics of core fractures in the Dingshan area.

field measurement was that after tectonic deformation of the stratum in the late period. Using the level calibration method, the dip angle variations and development situations of the conjugate joint before and after calibration were compared. The intersection line of the conjugated shear joint was parallel to the middle principal stress axis σ_2 , and the maximum principal stress axis σ_1 and the minimum principal stress axis σ_3 were respectively parallel to the angular bisector of its acute and obtuse angles, which determined the direction of the principal stress. In this study, strGraphPrj software was adopted to reconstruct the fracture occurrence, and the occurrence shape data of fractures after calibration were obtained (Qin Limao et al., 2003). Then, DIPS geological geometric analysis software was used to analyze the preferred orientation of fracture strike with rose diagrams and stereographic projection on the occurrence shape after reconstruction; thus, the direction the maximum principal stress was determined (Yang Weiran and Zhang Wenhui, 1996).

Based on the reconstruction of the fracture occurrence shape, combined with the intersected relation of the tectonic evolution characteristics with the outcrop fractures of the study area, the fractures were staged and matched (Table 1).

Plane shear fractures intersected with the vertical or high angles of the stratum surface. The fracture surface was straight and had a more stable appearance, which is often produced with a plane "X" conjugate; the section shear fractures were oblique to the rock plane at low angle, and the degree of development was poor relative to the plane shear fractures; tensile fractures were irregular in shape, with large variations in width and short extensions. According to the field fracture intersection relations and conjugate fracture recognition principles, the fracture data of the observation section was corrected for the stratum occurrence and then the fractures were staged and matched. The results showed that there were four groups of X-shaped plane conjugate shear fractures (Table 1) in shale of the Longmaxi Formation in the study area in the spatial distribution of structural fractures in the shale layer, with NWW ($295^\circ \pm 5^\circ$) and NNW directions ($345^\circ \pm 5^\circ$), which constituted an early X-shaped plane conjugate shear fracture. These two sets of fractures formed early and were formed by the strong thrust of SE from the SE to the NW in the Jiangnan Xuefeng uplift. At the later stage of the tectonic action, a section shear fracture with NNE ($35^\circ \pm 5^\circ$) and a small amount of NE tensile fractures were also formed. Near SN ($5^\circ \pm 5^\circ$) and NEE ($85^\circ \pm 5^\circ$) constituted another flat X-shaped conjugate shear fracture, which was formed by the extrusion in an NE direction, caused by the Central Sichuan, Jiangnan, and Central

Guizhou uplifts in the late Yanshanian-mid-Himalayan, slightly later than SEE and SSE toward the fractures. Under this tectonic movement, NW-direction ($315^\circ \pm 5^\circ$) shear fractures were also formed.

4.2.2 Description of Core observations imaging logging data to divide fracture phases

The research of core observation combined with imaging logging found that there were four groups of development directions of the tectonic fractures in the study area (Fig. 4); fractures of a NWW ($305^\circ \pm 5^\circ$) and NEE ($80^\circ \pm 10^\circ$) direction developed the most, followed by those of NNE ($30^\circ \pm 5^\circ$) and NNW ($350^\circ \pm 5^\circ$) directions, and those of NWW ($305^\circ \pm 5^\circ$) and NNW ($350^\circ \pm 5^\circ$) directions were of the same phase and could be matched to planar X-shaped conjugated shear fractures according to the intersected relations of core and fractures and the filling characteristics, whereas fractures of NNE ($30^\circ \pm 5^\circ$) and NEE ($80^\circ \pm 10^\circ$) directions could be matched to the planar X-shaped conjugated shear fractures of another phase, which was consistent with the earth surface shear fractures of the study area in both occurrence shape and staged match. Owing to restrictions of wellbore locations, wellbore size, and the FMI range, FMI logging data in each well only reflected the development of fractures around wellbores and could not fully reflect the overall development of the underground fracture. Although dominant fracture positions were different in each well, they should all be included in the fracture development azimuth observed at the surface; the borehole azimuth has certain correspondence with the surface fracture azimuth. It can be seen that the downhole and surface fractures were controlled by the same tectonic stress field, and the surface fractures were consistent with the underground fractures in the formation mechanism.

4.2.3 Description of downhole fault structure to analyze fracture phases

The evolution of the fault structure and development in the study area occurred under the control of the tectonic stress field in the southeastern Sichuan region, and they share certain inheritance and consistency in cause and characteristics. Therefore, the tectonic development phases could also be analyzed combined with the fault structure of the Longmaoxi Formation in the study area.

The geophysical explanation (Fig. 5) showed that the NE fault system dominated the Longmaxi Formation in the study area, followed by that of the NW and near SN directions. Most of the fault dip angles were above 30° to 60° , manifested as reverse faults of lower angles at the seismic section and formed under the effect of the tectonic stress of SE and NE directions; the fault of NE direction

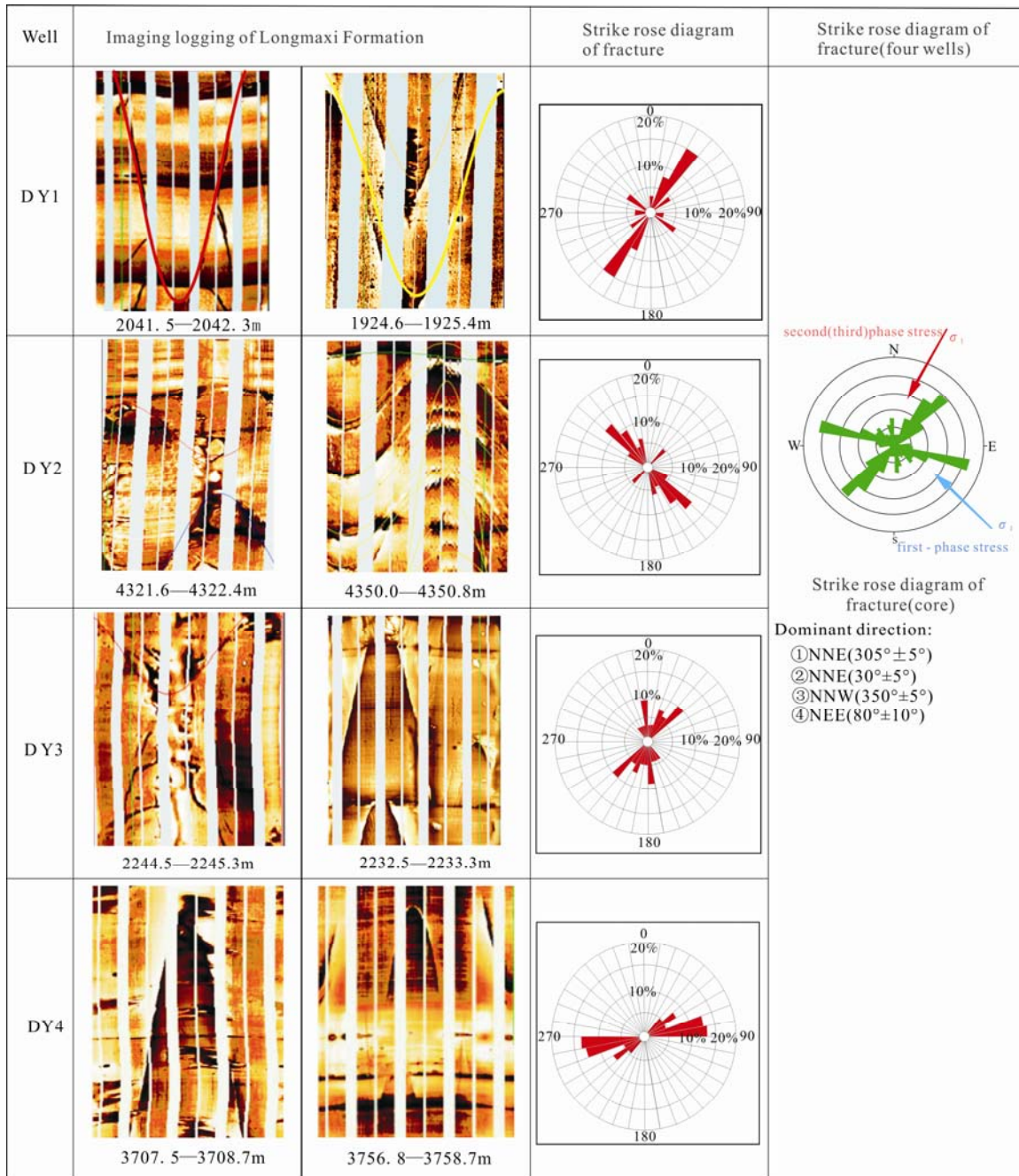


Fig. 4. Partial FMI logging and fracture attitude of the Longmaxi Formation.

was formed earlier than that of the NW and NW directions, and that of NW and near SN directions were formed later.

4.3 Experimental method

4.3.1 Homogenous temperature of fracture filling inclusions

According to the temperature distribution and its morphological characteristics of fractures in different phases, the major development phases of the tectonic fractures in this area were classified based on the revolution characteristics of Dingshan.

The test results of the inclusion samples of the filling fluid in the DY2 well fractures in Dingshan (Table 2; Fig. 6) suggest that there are at least three phases of fluid charging activities in the fractures of the Longma Formation shale, proving the existence of shale gas migration. Phase one corresponded to the first-phase tectonic uplift of the Dingshan area reaching the maximum burial depth, with the general homogenous temperature of 296–325°C and relatively high inclusion temperatures. Phase two occurred in the initial stage of the tectonic uplift, with the largely homogeneous temperature of 297–310°C, and the saltwater inclusions in both siliceous

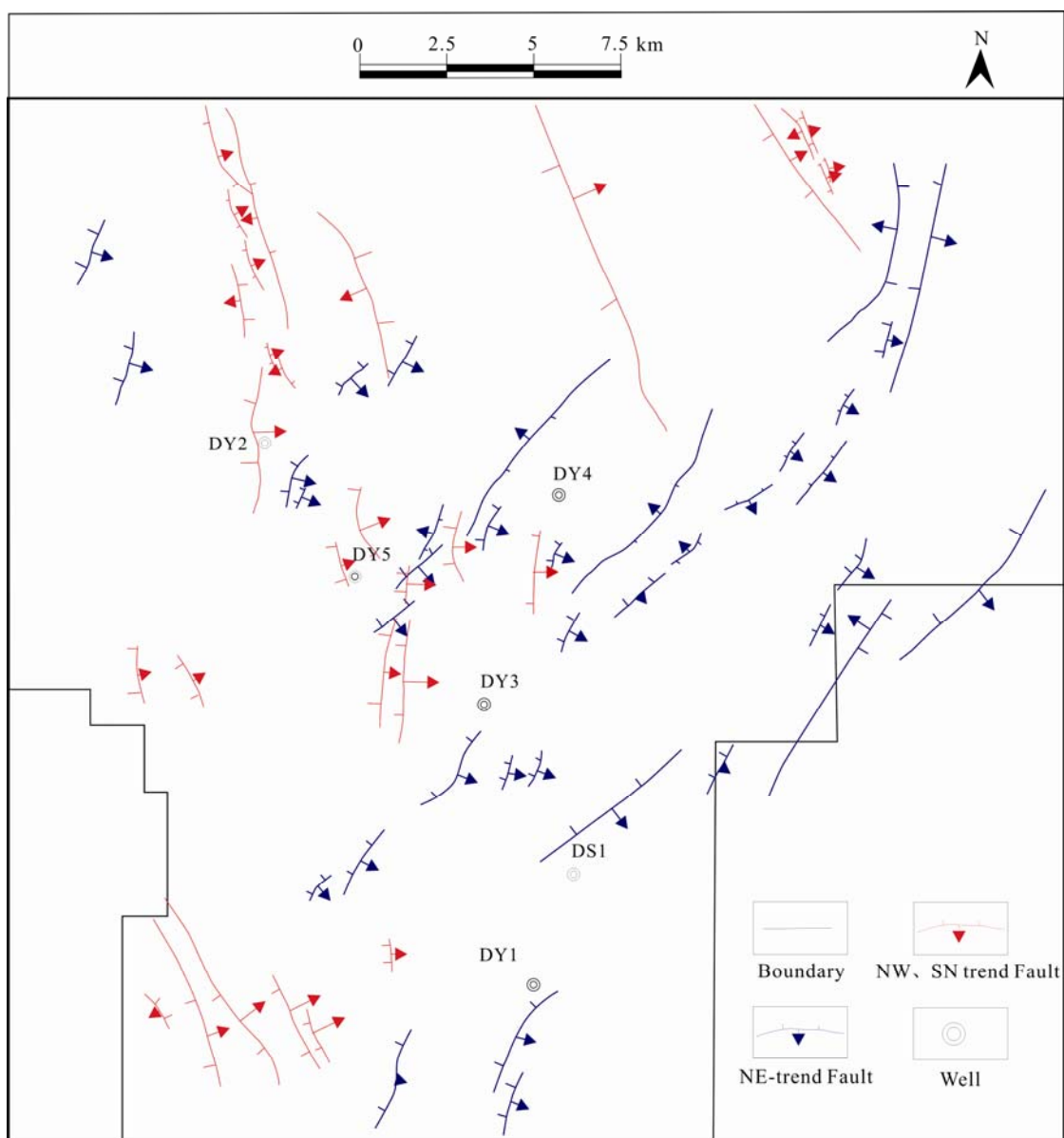


Fig. 5. Outline map of the fault system of the Longmaxi Formation in the Dingshan structure.

Table 2 Characteristics of fluid inclusions filled in shale fractures in the Dingshan area

Well location	Serial number	Horizon	Depth (m)	Homogenization temperature (°C)	Occurrence	Description of hand specimens	Host minerals
DY2	1	S ₁ /l	4,364	258.3	Primary	Black shale, high angle fracture filling with calcite veins	Calcite
	2	S ₁ /l	4,364	274.6	Primary	Black shale, high angle fracture filling with calcite veins	Calcite
	3	S ₁ /l	4,364	180.1	Primary	Black shale, high angle fracture filling with calcite veins	Calcite
	4	S ₁ /l	4,363.78	281.3	Primary	Black shale, high angle fracture filling with calcite veins	Calcite
	5	S ₁ /l	4,363.78	297.8	Primary	Black shale, high angle fracture filling with calcite veins	Calcite
	6	S ₁ /l	4,363.78	189.1	Primary	Black shale, high angle fracture filling with calcite veins	Calcite
	7	S ₁ /l	4,363.78	232.4	Primary	Black shale, high angle fracture filling with calcite veins	Calcite
	8	S ₁ /l	4,363.78	309.6	Primary	Black shale, high angle fracture filling with calcite veins	Calcite
	9	S ₁ /l	4,363.78	316.9	Primary	Black shale, high angle fracture filling with siliceous veins	Siliceous
	10	S ₁ /l	4,363.78	318.1	Primary	Black shale, high angle fracture filling with siliceous veins	Siliceous
	11	S ₁ /l	4,363.78	312.7	Primary	Black shale, high angle fracture filling with siliceous veins	Siliceous
	12	S ₁ /l	4,363.78	298.6	Primary	Black shale, high angle fracture filling with siliceous veins	Siliceous
	13	S ₁ /l	4,363.78	325.2	Primary	Black shale, high angle fracture filling with siliceous veins	Siliceous
	14	S ₁ /l	4,363.78	295.6	Primary	Black shale, high angle fracture filling with siliceous veins	Siliceous

cements and calcite cements showed relatively high temperatures, with a roughly coincident temperature range. However, the calcite could be seen crushed under

the microscope, and cemented by siliceous matters, which is formed after calcite. Therefore, the calcite cement settled in the first phase of fluid activities was gained,

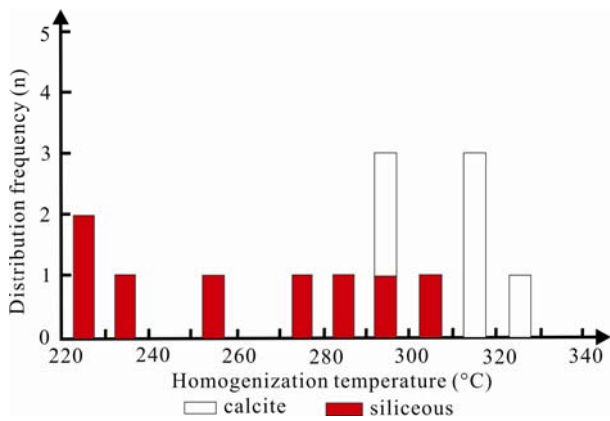


Fig. 6. Fluid activity phase histogram of the Longmax Formation in the DY2 well.

crushed in the later tectonic activities, and cemented by the siliceous matters settled in the second phase.

4.3.2 Apatite fission track and burial history analysis

The experimental analysis of the sample apatite fission track in the Dingshan area showed that (Fig. 7), a common law could be obtained from the apatite fission track *T-t* trajectories of the three samples that have very similar time transition points of the uplift and settlement. The three sample apatite fission tracks, selected from different locations and horizons showed a similar law, representing the uplift and settlement history of the Dingshan construction well. Since the middle to the late phase of the

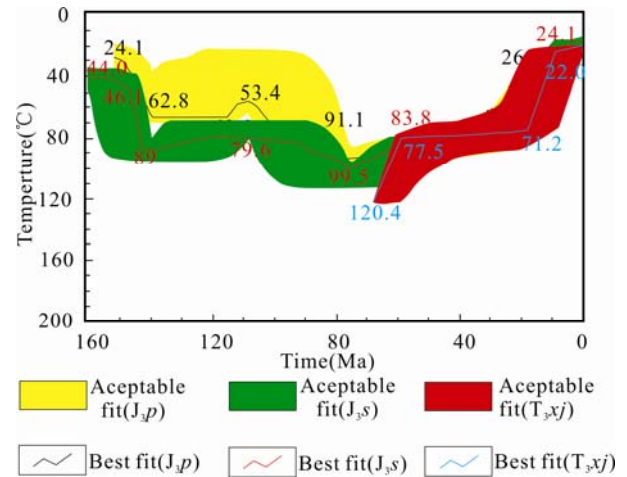


Fig. 7. The figure of apatite fission track temperature-time historical traces (after Wang Dong, 2009).

Yanshan tectonic movement (about 76 Ma), three obvious, two rapid, and a slow uplift have occurred in the study area.

The DY1 well, located in Shihao, Qijiang County, Chongqing, belongs to the Dingshan construction in the Lintanchang-Dingshan tectonic belt of a NE direction in the southeastern Sichuan area. The Lower Triassic Thatch Formation apatite was exposed on the ground surface, and the Upper Sinian Dengying Formation of the bottom drill passed. The burial history of DY1 well was amended (Ding Wenlong et al., 2012) (Fig. 8). The study area has

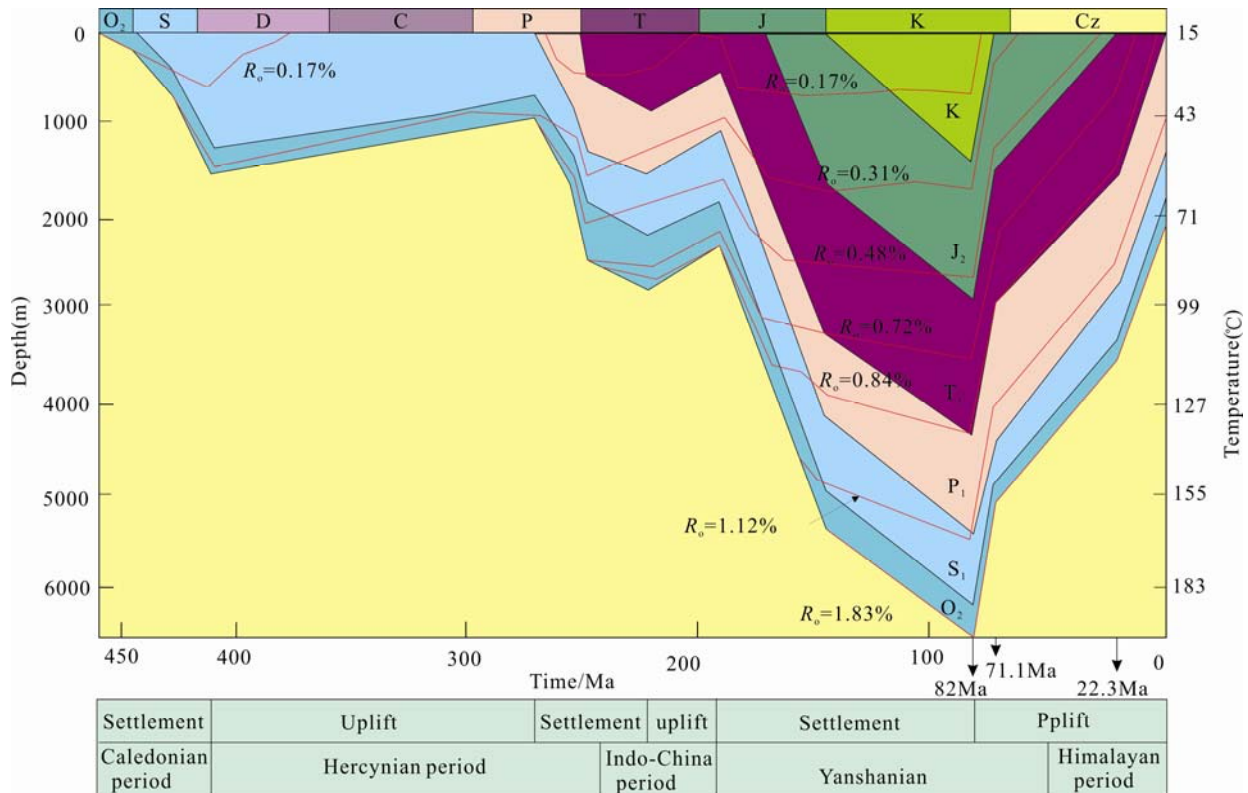


Fig. 8. The buried history of DY1 well in the Dingshan area (Nie Haikuang, 2016).

experienced three stages of tectonic uplift since the Yanshan tectonic movement: the first stage was in the middle-late phase of Yanshan movement (82–71.1 Ma), with the deepest burial after a rapid uplift; the second stage was at the end of Yanshan movement—the middle phase of Himalayan movement (71.1–22.3 Ma), experiencing a slow uplift; the third stage was in the middle phase of the Himalayan movement—present (22.3–0 Ma), being in the rapid uplift stage, with a short duration and weak impact.

4.3.3 Rock acoustic emission experiment

By summarizing and screening the data, it could be seen from the energy cumulative number-time relationship curve that with the gradual increase of load capacity a sharp increase occurred from 50, then four sharp energy cumulative increases occurred, resulting in a total of five energy cumulative heights (Fig. 9). There were five distinct inflection points on the energy cumulative percentage-time relationship curve, Kaiser effect feature points (Fig. 10). The sample acquisition horizon was located in the Longmaxi Formation at the downhole core (S_{1l}), and there were five Kaiser effect points on the energy cumulative number-time relationship curve and energy cumulative percentage-time relationship curve, corresponding to four obvious tectonic movements besides the current tectonic movement.

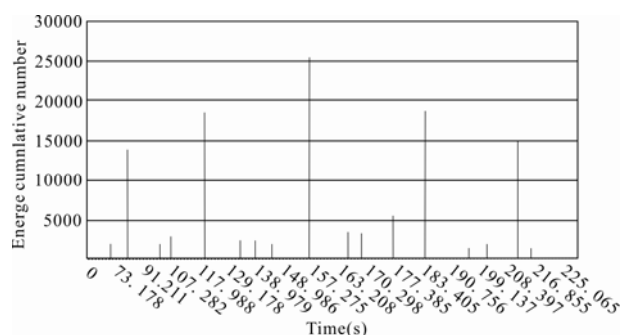


Fig. 9. Relationship of energy cumulative number with time for S_{1l} samples.

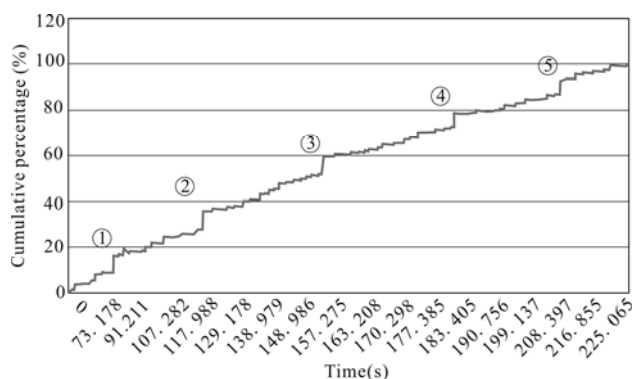


Fig. 10. Relationship of energy cumulative percentage with time for S_{1l} samples.

According to the original data of the acoustic emission experiment, the stress value, acoustic emission number and stress-time relationship curve of the rocks of various direction was obtained, and combined with the calculation formula of rock acoustic emission method (AES), the stress value at each sampling direction corresponding to the Kaiser point was determined (Table 3).

According to the acoustic emission experiment data, the following results were obtained: There were five Kaiser effect points in the Longmaxi Formation of the Dingshan area, which reflected that the rock experienced five microburst events in the geological history period. Combined with the existing research results and regional tectonic evolution history of the study area and surrounding area, the comprehensive analysis suggested that the five movement phases of the Longmaxi Formation rock corresponded to the current tectonic stress, the late phase of Himalaya, end of Yanshan—the mid-phase of Himalaya, mid-/late phase of Yanshan, and Indosinian, among which the movement at the Indosinian phase was an overall rise and fall tectonic movement, exerting a weak impact on the tectonic fracture and fold form.

In conclusion, the formation period of the Longmaxi Formation in the area was divided into three phases: the late phase of the Yanshan, end of the Yanshan—mid-phase of the Himalayan t, and late phase of the Himalayan movements. Specifically, the first phase was the middle and late period of the Yanshan tectonic movement, with a corresponding time of 82–71.1 Ma, and was mainly impacted by the squeezing effect of the Jiangnan Xuefeng uplift of a SE-NW direction, with a maximum effective principal stress of 72.62–83.5 MPa; the second phase was the end of the Yanshan movement—mid-phase of the Himalaya movement, and the corresponding time was 71.1–22.3 Ma, mainly impacted by the joint action of the Jiangnan Xuefeng, Chuanzhong, and Qianzhong uplifts, triggering the squeezing effect of the NE-SW direction, with a maximum effect principal stress value of 90.49–107.1 MPa; the third phase was the Himalayan movement—present, and the corresponding time was 22.3–0 Ma, which was also impacted continuously by the joint action of the Jiangnan Xuefeng, Chuanzhong, and Qianzhong uplifts, but the tectonic stress intensity was relatively low and unstable, with a short duration time. Therefore, the first and second phases were the main development

Table 3 Results of rock acoustic emission

Serial number	Well	Depth (m)	Stress component of the AE point			σ_H (MPa)	σ_h (MPa)
			0°	45°	90°		
1	DY3	2,215	72.08	50.46	64.28	107.10	70.81
2	DY4	3,729	70.41	48.64	56.36	90.49	60.82
3	DY4	3,715	72.97	49.65	56.43	102.56	68.22
4	DY4	3,625	66.86	47.80	55.25	96.54	67.60
5	DY2	4,355	73.83	52.83	59.31	105.21	74.13

phases, and in the third phase slight transformation and superposition were made to the existing structure.

5 Discussions

5.1 Cause judgment and exploration forecast based on the methods

Based on the study of field outcrops, core fractures

features, homogeneous temperature test of fracture filling, rock acoustic emission tests, and burial-thermal evolution history of the Longmaxi Formation in the study area, the formation model of the shale fractures of the Longmaxi Formation in the area were established (Fig. 11).

In the middle-late period (82–71.1 Ma) of the Yanshanian tectonic movement, the study area, impacted by the strong squeezing effect of SE to NW directions for

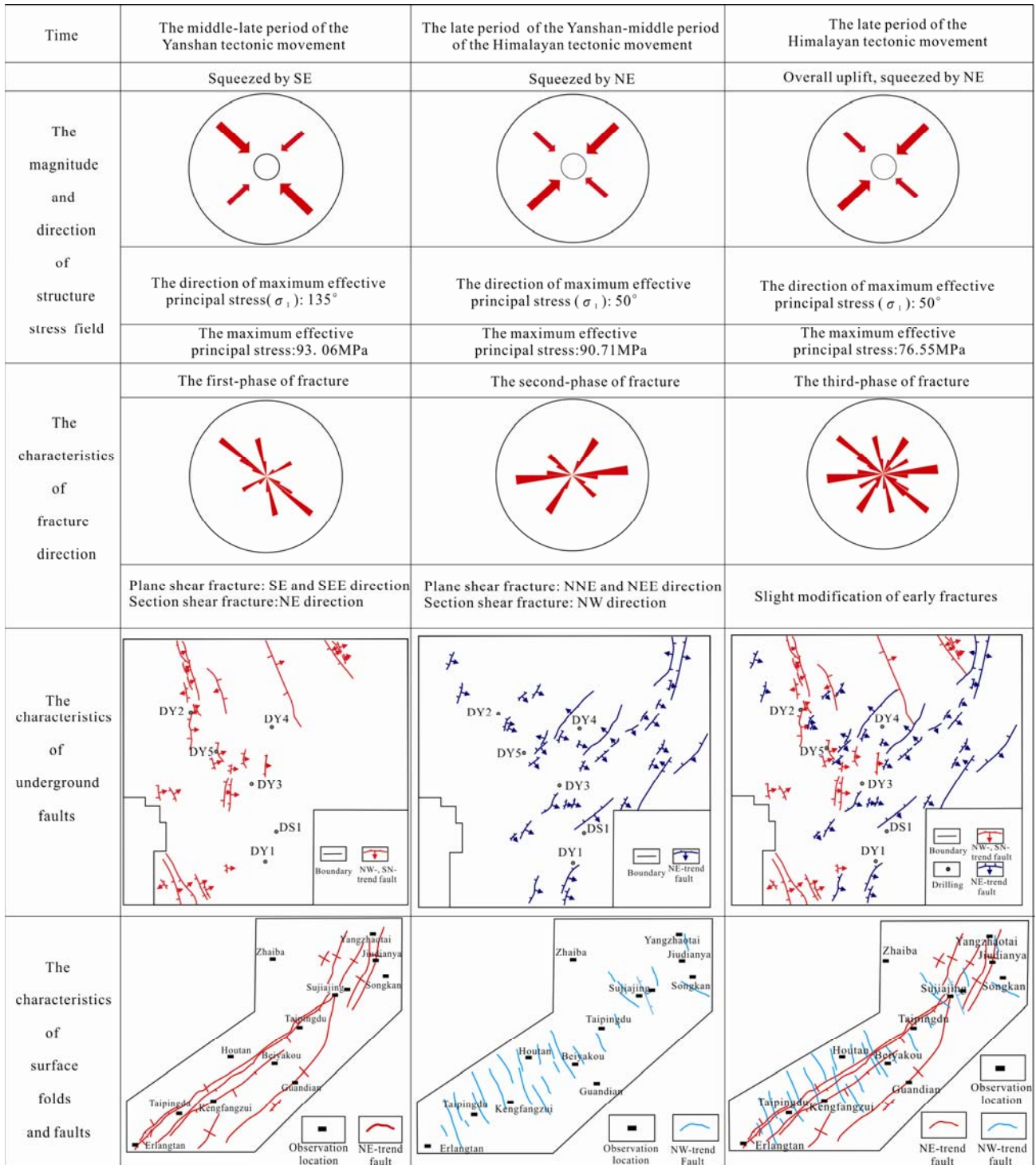


Fig. 11. Fracture mechanism of the Longmaxi Formation in the Dingshan area.

the continuous orogeny movement of the Jiangnan Xuefeng Mountain, had the principal stress of a SE-NW direction and, before the Longmaxi Formation stratum had obvious deformation, developed a group of planar X-shaped conjugated shear fractures, which were intersected with the stratum at high angles, with a fracture dip angle $>75^\circ$ and the main fracture direction of NWW-SEE and NNE-SSW, manifested on the plane as X-shaped conjugated shear fractures. This group of fractures were basically consistent with those found in investigations on ground surface fractures—fractures of NWW direction ($265^\circ \pm 5^\circ$) and NNW direction ($345^\circ \pm 5^\circ$) and those of NWW direction ($280^\circ \pm 5^\circ$) and NNW direction ($350^\circ \pm 5^\circ$) found in cores and imaging logging. Under the continuous squeezing of SE-NW directional stress, the NE-induced sectional shear fractures were further developed, finally into folds and fracture systems of a NE direction. This group of fracture fillings was formed the earliest, with the highest filling degree, and the filling was generally calcite, followed by siliceous matters and pyrite.

At the end of the Yanshan-mid-phase of the Himalayan movement (71.1–22.3 Ma), with the continuous action of the orogeny movement at the basin edge, the study area, affected by the double stress from the southeastern and northern regions (the combined effect of Jiangnan Xuefeng, Chuanzhong and Qianzhong uplift), had the principal stress of a NE-SW direction, forming planar X-shaped conjugated shear fractures of near SN and NEE directions. This group of fractures was basically consistent with those found in investigations on ground surface fractures – fractures of near SN direction ($345^\circ \pm 5^\circ$) and NEE direction ($80^\circ \pm 10^\circ$) and those of near SN direction ($0^\circ \pm 5^\circ$) and NE direction ($40^\circ \pm 10^\circ$) found in cores and imaging logging. Simultaneously, with the continual effect of the tectonic force of a NE direction, NW-trending sectional shear fractures perpendicular to the principal stress direction were formed in the fractured strata, and further expanded into a NW-trending fault system. This phase of fractures showed a low filling degree, and the filling was mainly calcite.

In the late stage of Himalayan movement-present (22.3–0 Ma), under the effect of the NE-trending tectonic and vertical stress, the strata of the Longmaxi Formation continued to fold and deform in local areas, and developed NW-trending sectional X-shaped shear fractures perpendicular to the principal stress direction. The fractures of this group were less developed, only locally developed, and not substantially filled. Simultaneously, the tectonic stress field renovated and superposed the earlier fracture system of NW and NE directions, and the composite fault system was formed in NW and NE directions in this area.

5.2 Rationality of methods

This study employed a method integrating qualitative geological analyses and quantitative experimental tests to determine fracturing and faulting episodes. The Longmaxi Formation in the Dingshan region of southeastern Sichuan Basin, China, was studied and satisfactory results were obtained.

Through geological field surveys of fractures, and comprehensive resolution of fractures in cores and resolution of faults, the development and formation episodes of fractures can be characterized by intuitive geological means. It is worth pointing out that faults are the products of further propagation of fractures, and resolution of faults can thereby facilitate the determination of fracturing episodes. Homogenization temperature tests on inclusions in fracture fillings, rock acoustic emission experiments, and burial/thermal history experiments, allow accurate quantification of various stages and ages of fracture formation and paleo-tectonic stresses at the time of fracture formation. This enables more detailed and quantitative findings of fracturing episodes and causes.

Doubtlessly, there is, to a certain degree, a different understanding of the experimental principles and results of both the geological and the quantitative analyses. For example, for the Kaiser effect points acquired through acoustic emission experiments, it is hard to decide to which tectonic movement episode each of them should correspond. Concerning the burial/thermal history analysis, the earliest tectonic uplift time found in this study is 71.1 Ma, while that by Wang et al. (2010) is 82 Ma, a difference of about 10 Ma. The tectonic episodes that these results are correlated with, however, are actually consistent. The only difference lies with the specific time of the tectonic activity, which may be due to factors such as selection of test samples and instrumental errors.

6 Conclusions

(1) The Longmaxi Formation in the Dingshan area mainly developed tectonic, diagenetic, and horizontal slip fractures. It was mainly comprised of high-angle shearing and horizontal slip fractures, with small opening, large spacing, low density, and high filling characteristics. After fracture correction, the dominant directions of fractures included NWW, near SN, NNW, NEE, near EW, and NW. Fracture intersection relationships were obvious: NWW and NNW fractures, and near SN and NEE fractures formed two groups of X-shaped plane conjugate shearing fractures, NEE-direction and NW-direction fractures constituted two sets of "X-shaped" section shearing fractures, and a small amount of NE-direction fractures were tensile fractures.

(2) Combining qualitative geological analysis with quantitative experimental testing methods, it was determined that fracture periods of the Longmaxi Formation in the Dingshan area were mainly divided into three phases: the first-phase of structural fractures formed during 82–71.1 Ma, with a high degree of calcite fillings, homogenization temperature of 295.6–325.2°C and maximum effective principal paleo-geological stress was 97.06 MPa. The second-phase of structural fractures formed during 71.1–22.3 Ma, with a high degree of calcite and siliceous fillings, homogenization temperature was 189.1–232.4°C and the maximum effective principal paleo-geostatic stress was 90.71 MPa. The third-phase of structural fractures formed during 22.3–0 Ma, and a small amount of fractures were developed with a low degree of calcite fillings. The maximum effective principal paleo-geostatic stress was 76.55 MPa.

(3) Tectonic fractures of the Longmaxi Formation in the Dingshan area were formed by the tectonic movements of middle-late Yanshanian, late Yanshanian-middle Himalayan, and late Himalayan movements. The first two tectonic movements were during the main forming time of fractures and tectonic systems. Tectonic movement since the late Himalayan tectonic movement mainly slightly modified and superimposed existing fractures and structural systems. Based on the principles of tectonic analysis and geomechanics, fracture formation models in the Longmaxi Formation in the Dingshan area were established, and the mechanism of fracture formations in the Longmaxi Formation was clarified. The research methods and results have important guiding significance for deepening the understanding of preservation conditions and promoting shale gas exploration and development.

Acknowledgements

This research was financially supported by the Open Fund (grant No. PLC 20180404) of State Key Laboratory of Oil and Gas Reservoir Geology and Exploitation, Chengdu University of Technology. We would like to express our gratitude to the two anonymous reviewers for their constructive suggestions and comments which have greatly improved the manuscript.

Manuscript received Dec. 21, 2017

accepted Jan. 15, 2018

edited by Hao Qingqing

References

- Ambrose, R.J., Hartman, R.C., Campos, M.D., Akkutlu, I.K., and Sondergeld, C., 2010. New Pore-scale Considerations for Shale Gas in Place Calculations. *Society of Petroleum Engineers*, 010: 219–229.
- Anderson, E.M., 1948. On lineation and petrofabric structure, and the shearing movement by which they have been produced. *Quarterly Journal of the Geological Society of London* 413(104, Part 1): 104: 99–132.
- Awdal, A.H., Braathen, A., Wennberg, O.P., and Sherwani, G.H., 2013. The characteristics of fracture networks in the Shiranish Formation of the Bina Bawi Anticline; comparison with the Taq Taq Fied, Zagros, Kurdistan, NE Iraq. *Petroleum Geoscience*, 19(2): 139–155.
- Bai Bin, Zou Caineng, Zhu Rukai, Zhang Bian, Zhang Benjian, Bi Lina and Su Ning, 2012. Characteristics and formation stage-times of structural fractures in tight sandstone reservoir on the 2nd member of Xujiahe Formation in southwestern Sichuan Basin. *Acta Geologica Sinica*, 86(11): 1841–1846 (in Chinese with English abstract)
- Bao Hongzhi, Sun Lianhuan, Yu Lingling and Zhang Huawei, 2009. Obtainment of ground stress by Kaiser effect of rock acoustic emission. *Fault-Block Oil & Gas Field*, 16(6): 94–96 (in Chinese with English abstract).
- Borjigin Tenger, Shen Baojian, Yu Lingjie, Yang Yunfeng, Zhang Wentao, Tao Cheng, Xi Binbin, Zhang Qingzhen, Bao Fang and Qin Jianzhong, 2017. Mechanisms of shale gas generation and accumulation in the Ordovician Wufeng-Longmaxi Formation, Sichuan Basin, SW China. *Petroleum Exploration and Development*, 44(01): 69–78 (in Chinese with English abstract).
- Bustin, R.M., 2005. Gas shale tapped for big pay. *AAPG Explorer*, 26(2): 5–7.
- Curtis, J.B., 2002. Fractured shale-gas systems. *AAPG Bulletin*, 86(11): 1921–1938.
- Dai Junsheng, Wang Yukun, Feng Jianwei, Li Shubo and Wang Yongjuan, 2017. Characteristics and formation periods of fractures in Ordovician carbonate rocks in Hetianhe gas field. *Xingjiang Petroleum Geology*, 38(2): 133–136 (in Chinese with English abstract).
- Dai Peng, Ding Wenlong, He Jianhua, Li Ang, Zhao Dong and Zhao Wei, 2015. Application of geophysical techniques in fracture of shale reservoir. *Progress in Geophysics*, 30(3): 1315–1328 (in Chinese with English abstract).
- Deng Bin, Liu Shu-gen, Yang Suo, Li Zhiwu and Zhao Jiancheng, 2009. Structural characteristics of Joints and its implication in the Lingtanchang Anticline. *J. Mineral Petrol*, 29(3): 83–90 (in Chinese with English abstract).
- Ding Wenlong, Li Chao, Li Chunyan, Xu Changchun, Jiu Kai, Zeng Weite and Wu Liming, 2012. Dominant factor of fracture development in shale and its relationship to gas accumulation. *Earth Science Frontiers*, 19(2): 212–220 (in Chinese with English abstract).
- Fan Cunhui and Qin Qirong, 2016. Characteristics and formation stages of the reservoir fractures of the Xujiahe Formation in the fault-fold belt of the central Yuanba area of the Sichuan Basin. *Journal of the Balkan Tribological Association*, 22(2): 1049–1062.
- Fan Cunhui and Qin Qirong, 2016. Tectonic fractures in tight sandstone reservoirs of the Upper Cretaceous Qingshaokou Formation in Yaoyingtai area of southern Songliao Basin, China. *Journal of the Balkan Tribological Association*, 22(3): 2640–2476.
- Fan Cunhui, Qin Qirong, Li Hu, Han Yutian and Xing Jiaxin, 2017. Formation stages of structural fractures of Xujiahe Formation in the fault-fold belt of central Yuanba area,

- Sichuan Basin. *Acta Petrolei Sinica*, 38(10): 1135–1143 (in Chinese with English abstract).
- Feng Dongjun, Hu Zongquan, Gao Bo, Peng Yongmin and Du Wei, 2016. Analysis of Shale Gas Reservoir-Forming Condition of Wufeng Formation-Longmaxi Formation in Southeast Sichuan Basin. *Geological Review*, 62(06): 1521–1532 (in Chinese with English abstract).
- Feng Ziqi, Liu Dan, Huang Shipeng, Wu Wei, Dong Dazhong, Peng Weilong and Han Wenxue, 2016. Carbon isotopic composition of shale gas in the Silurian Longmaxi Formation of the Changning area, Sichuan Basin. *Petroleum Exploration and Development*, 43(05): 705–713 (in Chinese with English abstract).
- Gale, J.F.W., Laubach, S.E., Olson, J.E., Eichhubl, P., and Fall, A., 2014. Natural fractures in shale: a review and new observations. *AAPG Bulletin*, 98(11): 2016–2216.
- Guo Xusheng, Hu Dongfeng, Li Yuping, Liu Ruobing and Wang Qingbo, 2014. Geological features and reservoiring mode of shale gas reservoirs in Longmaxi Formation of the Jiaoshiba area. *Acta Geologica Sinica* (English Edition), 88(06): 1811–1821.
- Hao, F., Zou, H.Y., and Lu, Y.C., 2013. Mechanisms of shale gas storage: Implications for shale gas exploration in China. *AAPG Bulletin*, 99(8): 1325–1346.
- Hu Dongfeng, Zhang Hanrong, Ni Ka and Yu Guangchu. 2014. Main controlling factors for gas preservation conditions of marine shales in southeastern margins of the Sichuan Basin. *Natural Gas Industry*, 34(6): 17–23 (in Chinese with English abstract).
- Jarvie, D.M., Hill, R.J., Ruble, T.E., and Pollastro, R.M., 2017. Unconventional shale-gas systems: the Mississippian Barnett Shale of north-central Texas as one model for thermogenic shale-gas assessment. *AAPG Bulletin*, 91(4): 475–499.
- Larsen, B., Grunnaleite, I., and Gudmundsson, A., 2010. How fracture systems affect permeability development in shallow-water carbonate rocks: an example from the Gargano Peninsula, Italy. *Journal of Structural Geology*, 32(9): 1212–1230.
- Li Yang, Jin Qiang, Zhong Jianhua and Zou Shengzhang, 2016. Karst zonings and fracture-cave structure characteristics of Ordovician reservoirs in Tahe oilfield, Tarim Basin. *Acta Petrolei Sinica*, 37(3): 289–298 (in Chinese with English abstract).
- Li Yufeng, Sun Wei, Liu Xiwu, Zhang Dianwei, Wang Yanchun and Liu Zhiyuan, 2018. Study of the relationship between fractures and highly productive shale gas zones, Longmaxi Formation, Jiaoshiba area in eastern Sichuan. *Petroleum Science*, 15:498–509.
- Li Zhongquan and Liu Shun, 2010. Tectonic Geology. 3rd Edition. Beijing: *Geological Publishing House*, 96–117 (in Chinese).
- Lü Jing, Zhou Wen, Xie Runcheng, Shan Yuming, Zhang Chong and Xu Hao. 2017. Three-dimensional in situ stress-field simulations of shale gas formations: a case study of the 5~(th) member of the Xujiahe Formation in the Xinchang gas field, west Sichuan Depression. *Acta Geologica Sinica* (English Edition), 91(2): 617–629.
- Lu Yingxin, Hu Wangshui, Tang Jigunag, Zhang Qiong, Zhan Wen, Xiong Ping and Lv Hengyu, 2016. Development and distribution of fractures in Longmaxi Shale Formation of Dingshan structure in east. *Journal of Yangtze University* (Natural Science Edition), 13(8): 6–10 (in Chinese with English abstract).
- Martinesu, D.F., 2007. History of the Newark East Field and the Barnett Shale as a gas reservoir. *AAPG Bulletin*, 91(4): 399–403.
- Montgomery, S.L., Jarvie, D.M., Bowker, K.A., and Pollastro, R.M., 2005. Mississippian Barnett Shale, Fort Worth Basin, north-central Texas: gas-shale play with multi-trillion cubic foot potential. *AAPG Bulletin*, 90(6): 963–966.
- Nai Shenghua, Xu Qian, Zhou Wen and Sun Laixi, 2004. Development periods of fractures in the late Triassic-Jurassic in the north Chuxiong Basin. *Petroleum Exploration and Development*, 31(5): 25–29 (in Chinese with English abstract).
- Narr, W., 1991. Fracture density in the deep subsurface: techniques with application to Point Arguello Oil Field. *AAPG Bulletin*, 75(8): 1300–1323.
- Nelson, R.A., 2001. Geologic analysis of naturally fractured reservoirs (Second edition). *Gulf Professional Pub*, 1–332.
- Nelson, R.A., 2011. Geologic analysis of naturally fractured reservoirs: Contributions in petroleum geology and engineering. *Boston: Gulf Publishing*, 66–94.
- Newton, R.C., 1990. Fluid and shear zones in the deep crust. *Tectonophysics*, 182: 22–37.
- Nie Haikuang and Zhang Jinchuan, 2012. Shale gas accumulation conditions and gas content calculation: a case study of Sichuan Basin and its periphery in the Lower Paleozoic. *Acta Geologica Sinica*, 86(02): 349–361 (in Chinese with English abstract).
- Niu Hairui, Yang Shaochun, Wang Yong, He Niqian and Ma Baoquan, 2017. Analysis on the formation periods of fracture of volcanic reservoirs in Chepaizi area, Junggar Basin. *Natural Gas Geoscience*, 28(1): 74–84 (in Chinese with English abstract).
- Pedersen, T.F., and Calvert, S.E., 1990. Anoxia vs productivity: What controls the formation of organic-carbon-rich sediments and sedimentary rock. *AAPG Bulletin*, 74(4): 454–466.
- Qin Limao, Liu Yuanchao, Wu Dechao, Deng Hongjiang, Wang Daoyong and Xiao Yuanfu, 2003. The features and analysis of joints in Xiluodu area. *J. Mineral Petrol*, 3(23): 51–54 (in Chinese with English abstract).
- Ren Lihua and Lin Chengyan, 2007. Classification methods for development period of fractures and its application: a case study from Budate Group of Hailaer Basin. *Acta Sedimentologica Sinica*, 25(2): 253–260 (in Chinese with English abstract).
- Rodriguez, N.D., and Philp, R.P., 2010. Geochemical characterization of gases from the Mississippian Barnett Shale, Fort Worth Basin, Texas. *AAPG Bulletin*, 94(11): 1641–1656.
- Sonntag, R., Evans, J.P., and La, Pointe, P., 2012. Sedimentological control on the fracture distribution and network development in Mesaverde Group sandstone Lithofacies, Uinta Basin, Utah, USA. *Geological Society London Special Publication*, 374(1): 23–50.
- Sun Wei, Liu Shugen, Xu Guoshen, Wang Guozhi, Yuan Haifeng and Huang Wenming, 2010. Petroleum formed condition and process research for Sinian to Low Paleozoic at Dingshan structure in southeast of Sichuan Basin. *Geological Science and Technology Information*, 29(1): 49–55 (in Chinese with English abstract).
- Wang Ke, Zhang Huiliang, Zhang Ronghu, Wang Junpeng, Dai

- Junsheng and Yang Xuejun, 2016. Characteristics and influencing factors of ultra-deep tight sandstone reservoir structural fracture: a case study of Keshen-2 gas field, Tarim Basin. *Acta Petrolei Sinica*, 37(6): 715–727 (in Chinese with English abstract).
- Wang Ruyue, Ding Wenlong, Zhang Yejian, Wang Zhe, Wang Xinghua, He Jianhua, Zeng Weite and Peng Dai, 2016. Analysis of developmental characteristics and dominant factors of fractures in Lower Cambrian marine shale reservoirs: A case study of Niutitang formation in Cen'gong block, southern China. *Journal of Petroleum Science and Engineering*, 138: 31–49 (in Chinese with English abstract).
- Xu Kangkang, Du Yangsong, Cao Yi, Zhang Aiping and Luo Gan, 2012. Research on Palaeotectonic stress field and its evolution in Fanchang area, Anhui Province. *Geoscience*, 26(3): 498–507 (in Chinese with English abstract).
- Yan Changhong, Xu Xiaofeng and Zheng Yanglin. 2013. Research status and discussion of rock Kaiser effect in determining ground stress. *Journal of Gansu Sciences*, 25(3): 27–31 (in Chinese with English abstract).
- Yang Wei ran and Zhang Wen huai. 1996. Character of fault property and combination of fluid inclusions. *Earth Science-Journal of China University of Geosciences*, 21(3): 285–290 (in Chinese with English abstract).
- Yuan Haifeng, 2008. The mechanism of hydrocarbon accumulation, Sinian-Lower Palaeozoic Basin. *Chengdu University of Technology* (Ph. D thesis): 1–188 (in Chinese with English abstract).
- Yuan Yusong, Jin Zhijun, Zhou Yan, Liu Junxin, Li Shuangjian, Liu Quanyou. 2017. Burial depth interval of the shale brittle-ductile transition zone and its implications in shale gas exploration and production. *Petroleum Science*, 14:637–647.
- Zhang Jinhang, Zhao Qihua, Lv Tao, Luo Yong and Liu Yubin, 2010. Experimental research on measurement of in-situ stress by using Kaiser effect. *Journal of Xi'an University of Science and Technology*, 30(2): 207–211 (in Chinese with English abstract).
- Zhang Xuefen, Lu Xiancai, Zhang Linye and Liu Qin, 2010. Occurrences of shale gas and their petroleum geological significance. *Advances in Earth Science*, 25(6): 597–604 (in Chinese with English abstract).
- Zhao Jianhua, Jin Zhijun, Jin Zhenkui, Wen Xin and Geng Yikai. 2016. Physical mechanism of organic matter-mineral interaction in Longmaxi Shale, Sichuan Basin, China. *Acta Geologica Sinica* (English Edition), 90(05):1923–1924.
- Zheng Rongcai. 1998. A new method of studying reservoir fractures: acoustic emission experiment. *Oil & Geology*, 19(3):186–189 (in Chinese with English abstract).
- Zou Caineng, Dong Dazhong, Wang Yuman, Li Xinjing, Huang Jinliang, Wang Shufen, Guan Quanzhong, Zhang Chenchen, Wang Hongyan, Liu Honglin, Bai Wenhua, Liang Feng, Lian Wen, Zhao Qun, Liu Dexuan, Yang Zhi, Liang Pingping, Sun Shasha and Qiu Zhen, 2016. Shale gas in China: characteristics, challenges and prospects (II). *Petroleum Exploration and Development*, 43(2): 166–178 (in Chinese with English abstract).
- Zou Caineng, Yang Zhi, Pan Songqi, Chen Yanyan, Lin Senhu, Huang Jinliang, Wu Songtao, Dong Dazhong, Wang Shufang, Liang Feng, Sun Shasha, Huang Yong and Weng Dingwei. 2016. Shale gas formation and occurrence in China: an overview of the current status and future potential. *Acta Geologica Sinica* (English Edition), 90(04):1249–1283.
- Zou Caineng, Yang Zhi, Zhu Rukai, Zhang Guosheng, Hou Lianhua, Wu Songtao, Tao Shizhen, Yuan Xuanjun, Dong Dazhong, Wang Yuman, Wang Lan, Huang Jinliang and Wang Shufang. 2015. Progress in China's unconventional oil & gas exploration and development and theoretical technologies. *Acta Geologica Sinica* (English Edition), 89(03): 938–971.
- Zumberge, J., Ferworn, K., and Brown, S., 2012. Isotopic reversal ('rollover') in shale gases produced from the Mississippian Barnett and Fayetteville Formation. *Marine & Petroleum Geology*, 31(1): 43–52.

About the first author

FAN Cunhui, male, born in 1980, is an instructor of Structural Geology in the School of Geoscience and Technology, Southwest Petroleum University. He received his M.S. degree in Southwest Petroleum University and his Ph.D. in Chengdu University of Technology. His main research directions are tectonic stress field and fractured reservoir characterization. E-mail:fanchswpi@163.com.